Conformational Analysis

Deutsche Ausgabe: DOI: 10.1002/ange.201410502
Internationale Ausgabe: DOI: 10.1002/anie.201410502

Evidence for a Boat Conformation at the Transition State of GH76 α-1,6-Mannanases—Key Enzymes in Bacterial and Fungal Mannoprotein Metabolism**

Andrew J. Thompson, Gaetano Speciale, Javier Iglesias-Fernández, Zalihe Hakki, Tyson Belz, Alan Cartmell, Richard J. Spears, Emily Chandler, Max J. Temple, Judith Stepper, Harry J. Gilbert, Carme Rovira, Spencer J. Williams,* and Gideon J. Davies**

Abstract: *α-Mannosidases and α-mannanases have attracted attention for the insight they provide into nucleophilic substitution at the hindered anomeric center of α-mannosides, and the potential of mannosidase inhibitors as cellular probes and therapeutic agents. We report the conformational itinerary of the family GH76 α-mannanases studied through structural analysis of the Michaelis complex and synthesis and evaluation of novel aza/imino sugar inhibitors. A Michaelis complex in an $^{O}S_2$ conformation, coupled with distortion of an azasugar in an inhibitor complex to a high energy $B_{2,5}$ conformation are rationalized through ab initio QM/MM metadynamics that show how the enzyme surface restricts the conformational landscape of the substrate, rendering the $B_{2,5}$ conformation the most energetically stable on-enzyme. We conclude that GH76 enzymes perform catalysis using an itinerary that passes through $^{O}S_2$ and $B_{2,5}^{\ddagger}$ conformations, information that should inspire the development of new antifungal agents.*

Enzymes catalyzing the hydrolysis of glycosidic bonds within α-mannoside-based glycans and glycoconjugates (α-mannosidases and α-mannanases) are of great interest due to their roles in glycoprotein maturation,[1] cell wall assembly in fungi,[2] and processing of complex dietary polysaccharides by the human gut microbiota.[3] Relatively little attention has been directed at *endo*-acting α-mannosidases and α-mannanases, enzymes that play major roles in eukaryotic N-glycan processing[4] and in the metabolism and deconstruction of fungal cell wall α-mannans.[3] *Endo*-α-mannanases are grouped into two families within the CAZy[5] sequence-based classification (http://www.cazy.org): GH99, which includes both mammalian and bacterial *endo*-α-mannosidases and *endo*-α-mannanases; and GH76, featuring *endo*-acting bacterial α-1,6-mannanases[3,5] and fungal transglycosidases.[2,6] A growing body of literature has reported detailed characterization of various GH99 *endo*-α-mannosidases in terms of function,[4a] cellular localization,[7] structure,[8] and the development of effective inhibitors that are active within cells;[9] by comparison our knowledge and understanding of the biological role of GH76 enzymes has trailed. While several GH76 structures are available, less is known of the biochemistry and mechanism of these enzymes, no inhibitors have been reported and nothing is known of the conformational changes occurring during catalysis.

Most α- and β-mannosidases perform catalysis through one of two conformational itineraries. X-ray structures of insightful ligand complexes, dovetailed with computational analyses of conformational free-energy landscapes (FEL) of inhibitors on- or off-enzyme, have allowed assignment of an $^{O}S_2 \leftrightarrow B_{2,5}^{\ddagger} \leftrightarrow {}^{1}S_5$ itinerary to α- and β-mannosidases of families GH2, 26, 38, 92, and 113.[10] Alternatively, an unusual "southern hemisphere" itinerary, $^{3}S_1 \rightarrow {}^{3}H_4^{\ddagger} \rightarrow {}^{1}C_4$, has been assigned to *exo*-acting α-mannosidases of family GH47.[11] Much effort has gone into the synthesis of enzyme inhibitors that either report on, or reflect, these conformational pathways. We recently provided evidence that the mannosidase inhibitor, mannoimidazole, is an exquisitely informative conformational probe, owing to the relatively small energy differences and barrier-less interconversion between ground-state $^{4}H_3$ or $^{3}H_4$ conformations, and higher energy $^{2,5}B$ or $B_{2,5}$ conformations.[10e] In contrast, the azasugar isofagomine

[*] Dr. A. J. Thompson, R. J. Spears, E. Chandler, Dr. J. Stepper, Prof. G. J. Davies
Department of Chemistry, University of York
Heslington, York, YO10 5DD (UK)
E-mail: gideon.davies@york.ac.uk
G. Speciale, Z. Hakki, T. Belz, Dr. A. Cartmell, Prof. S. J. Williams
School of Chemistry and Bio21 Molecular Science and Biotechnology Institute, University of Melbourne
Parkville, Vic 3010 (Australia)
E-mail: sjwill@unimelb.edu.au
J. Iglesias-Fernández, Prof. C. Rovira
Departament de Química Orgànica and Institut de Química Teòrica i Computacional (IQTCUB), Universitat de Barcelona
08028 Barcelona (Spain)
E-mail: c.rovira@ub.edu
M. J. Temple, Prof. H. J. Gilbert
Institute for Cell and Molecular Biosciences
The Medical School
Newcastle University, Newcastle upon Tyne, NE2 4HH (UK)

[**] We thank the Australian Research Council, the UK Biotechnology and Biological Sciences Research Council, Amicus Therapeutics, the Spanish Ministry of Economy and Competitiveness, the Generalitat de Catalunya, and the European Research Council. We also acknowledge the staff of the Diamond Light Source (Didcot (UK)) for provision of beamline facilities, and the support, technical expertise, and assistance provided by the Barcelona Supercomputing Center: Centro Nacional de Supercomputación. Supporting information for this article is given via a link at the end of the document.

Supporting information for this article is available on the WWW under http://dx.doi.org/10.1002/anie.201410502.

(IFG) was highlighted as a much poorer conformational probe owing to a greater preference for the ground-state $^4C_1$ conformation, and high-energy barriers that must be crossed to attain mechanistically relevant half-chair or boat conformations.[10e] In corollary, when a nonchair conformation is observed for IFG-type inhibitors bound to a glycosidase, this should be considered highly significant, with the conformational preferences of the enzyme overwhelming the otherwise dominating intrinsic conformational bias of the inhibitor.

Here, we performed a detailed mechanistic, structural, and conformational analysis of the catalytic domain of *Bacillus circulans* Aman6 (herein termed *Bc*GH76; see the Supporting Information (SI) for details), the founding member of the GH76 family of α-mannanases.[12] Three-dimensional (3D) structural analysis of the enzyme in diverse complexes at near atomic resolution reveals details of the catalytic conformational itinerary. Significantly, the Michaelis (enzyme-substrate) complex shows that the active center mannoside is distorted to an $^OS_2$ skew-boat conformation whilst a complex with the bespoke α-1,6-mannanase-targeted inhibitor 1,6-ManIFG **3** shows mechanistically relevant distortion, with the piperidine ring adopting a high-energy $B_{2,5}$ conformation. QM/MM metadynamics simulations show how the isolated mannoside[11b] and IFG free-energy landscapes[10e] are strongly perturbed on-enzyme, favoring *Bc*GH76 catalysis through a $B_{2,5}$ transition state ($TS^{\ddagger}$) conformation.

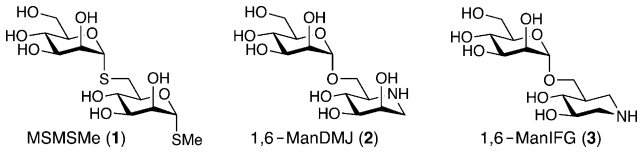

Consistent with previous reports,[12a] *Bc*GH76 is inactive against α-1,6-mannobiose (ManMan) and *p*-nitrophenyl α-mannoside (pNPMan); however, kinetic parameters could be determined using *p*-nitrophenyl α-1,6-mannobioside (pNPMan$_2$, $k_{cat}/K_M = 1.11\ min^{-1}\,mM^{-1}$) and α-1,6-mannotriose (α-1,6-Man$_3$, $k_{cat}/K_M = 27.7\ min^{-1}\,mM^{-1}$; see SI for details). Unlike various *exo*-mannosidase families (compare GH families 38, 47, and 92),[13] which employ divalent metal ions to coordinate and distort the geometry of the substrate, *Bc*GH76 is metal-independent, with no change in enzymatic activity in the presence of EDTA, and no evidence of metal ion coordination in any structures determined.

The 3D structure of wild-type *Bc*GH76 in complex with MSMSMe **1**, 1,6-ManDMJ **2**, and 1,6-ManIFG **3** were solved to resolutions of 1.30, 1.30, and 1.40 Å, respectively, whilst the structure of the *Bc*GH76-D125N variant in complex with α-1,6-mannopentaose was solved at 1.20 Å (Table S1). Consistent with other released GH76 structures (including a lower-resolution structure of WT *Bc*GH76 (PDB ID: 4BOK[14]) and a complex with α-1,6-mannobiose (4BOJ[14])) the native structure of *Bc*GH76 comprises an $(\alpha/\alpha)_6$ helical barrel fold with a long solvent-accessible cleft running laterally across the face of the barrel (Figure 1). Complexes with a kinetically identical engineered crystal-packing *Bc*GH76 variant (see SI) allowed identification of the active site and −4 to +1 sugar-

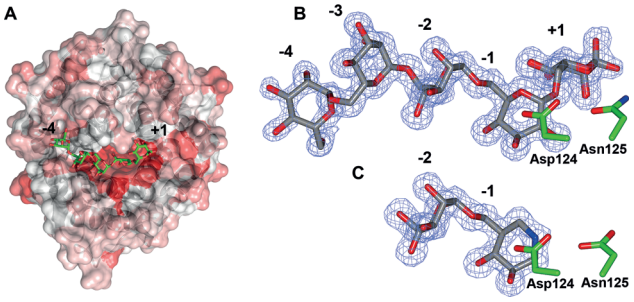

Figure 1. Three-dimensional structure, sequence conservation, and active site of GH76 α-1,6-mannanases. A) *B. circulans* TN-31 Aman6 catalytic domain (*Bc*GH76) in complex with α-1,6-mannopentaose with surface colored by sequence conservation using the partial GH76 alignment as shown in Figure S5. B) Complex with α-1,6-mannopentaose showing proposed catalytic nucleophile (Asp124) and general acid/base variant (Asn125). C) Complex with ManIFG **3**. Electron density maps are *REFMAC* maximum-likelihood/σ_A-weighted $2F_o-F_c$ syntheses contoured at 0.36 and 0.41 electrons per Å^3, respectively. Panel A was assembled using *PyMOL v1.6* (Schrödinger), panel B was assembled using *CCP4mg*.[17]

binding subsites (Figure 1; for subsite nomenclature see Ref. [15]). Both **1** and **2** bound in similar positions (−3/−2) away from the active center (see SI). In contrast, the Michaelis complex with α-1,6-mannopentaose spans the complete active center from −4 to +1 and shows distortion of the −1 subsite mannoside to an $^OS_2$ conformation; highly indicative[10b,c,16] of a $^OS_2 \leftrightarrow B_{2,5}^{\ddagger} \leftrightarrow {}^1S_5$ conformational pathway for GH76 catalysis. 1,6-ManIFG **3** binds to *Bc*GH76 with $K_d = 1.1\ \mu M$ (see SI), some 5000 times stronger than the K_M for pNPMan$_2$, and occupies the (−2/−1) subsites. Notably, the *Bc*GH76-**3** complex shows a distortion of the −1 moiety to a $B_{2,5}$ conformation (discussed below).

The structures of the Michaelis and *Bc*GH76-**3** complexes provide the first examples of a GH76 enzyme with ligands bound at the −1 subsite. GH76 enzymes act with a net retention of anomeric configuration,[3] consistent with catalysis using a classical Koshland double displacement mechanism. In the *Bc*GH76-**3** complex the endocyclic nitrogen of IFG (equivalent to the anomeric carbon) engages in a close contact (2.8 Å) with Asp124, congruous with other complexes of IFG-type sugars with retaining glycosidases (see SI). In the Michaelis complex Asp124 is poised for in-line nucleophilic attack on the anomeric center of the substrate with O_{nuc}–C1 distance 3.14 Å and an O_{nuc}-C1-O_{LG} angle of 160°. The neighboring amino acid, Asp125, occupies a position consistent with that of an *anti*-protonating general acid/base residue and is H-bonded to the leaving group glycosidic oxygen within the Michaelis complex. These structure-based assignments were investigated by mutagenesis. *Bc*GH76 D124N showed no activity against either pNPMan$_2$ or α-1,6-Man$_3$, consistent with its role as a catalytic nucleophile. As expected, a D125N variant was inactive toward α-1,6-Man$_3$ due to the requirement for general acid catalysis.

The conformational distortions observed in both the Michaelis and *Bc*GH76-**3** complexes are indicative of a $^OS_2 \leftrightarrow B_{2,5}^{\ddagger} \leftrightarrow {}^1S_5$ conformational pathway for *Bc*GH76 catalysis. Ab initio QM/MM metadynamics simulations were

used to quantify how *Bc*GH76 alters the preferences of both α-mannose and IFG for these higher energy conformers. The calculations show that the enzyme dramatically reshapes the energetically accessible conformational landscape of both the mannose[11b] and IFG[10e] moieties within the −1 subsite (Figure 2). Of special note, the undistorted $^4C_1$ conformers are no longer the global energy minima, and are situated at much higher energies than the most stable distorted conformation (6 kcal mol^{-1} higher compared to the $^NS_5/B_{2,5}$ conformer of IFG and >15 kcal mol^{-1} higher compared to the $^OS_2/B_{2,5}$ conformer of the α-mannoside at the −1 subsite in the Michaelis complex). In sum, these data are consistent with GH76 enzymes acting through a canonical $^OS_2 \leftrightarrow B_{2,5}^{\ddagger} \leftrightarrow {}^1S_5$ itinerary (Figure 3).

An unexpected interaction, apparently unique to *Bc*GH76, is observed within the Michaelis and *Bc*GH76-**3** complexes. In both structures the catalytic nucleophile (Asp124) makes a direct hydrogen bonding interaction with the distal 3-OH group of the substrate and inhibitor (O–O distance approx. 2.7 Å, see Figures 1 and S4). These interactions are also predicted for the lowest-energy conformations of the on-enzyme FELs for α-mannose and IFG (Figure 2). Hydrogen-bonding interactions with the −1 sugar 2-hydroxy and the nucleophile of retaining β-glucosidases/β-xylanases have been shown to be important for catalysis, contributing up to 10 kcal mol^{-1} to TS‡ stabilization.[18] In the case of α-mannosidases with the −1 sugar in an $^OS_2$ conformation in the Michaelis complex, the 3-hydroxy group is geometrically positioned to provide a similar interaction, and we speculate that this hydrogen bonding interaction facilitates deformation to a reactive $^OS_2$ conformation in the Michaelis complex, and is geometrically and electronically optimized to stabilize the $B_{2,5}$ TS‡. Notably, such an interaction is not possible for retaining β-mannosidases as the catalytic nucleophile approaches the anomeric position from the opposing (bottom) face of the substrate. Furthermore, such an interaction is not possible for the metal-dependent α-mannosidases of families GH38, 47, and 92, as the essential divalent metal (Ca^{2+} or Zn^{2+}) bridges O2 and O3, which has been speculated to assist distortion of the substrate into the preactivated conformation required for catalysis, assist in conformational transitions along the reaction coordinate,[10d] and stabilize charge development on O2 at the TS‡.[19] Interestingly, an analogous interaction is present within family GH38 enzymes in which the catalytic nucleophile makes a direct interaction with Zn^{2+}.[19] Intriguingly, this interaction has remarkable precedent in a chemical glycosylation involving the nucleophilic substitution of a 4,6-benzylidene-protected α-mannosyl triflate; density functional theory calculations of the TS‡ based on kinetic isotope effects implicated a $B_{2,5}$ conformation characterized by the presence of a hydrogen bond between the acceptor alcohol and O3 of the donor.[20]

Previous work has suggested that IFG-type inhibitors, which thus far have only been observed in $^4C_1$ conformations when bound to mannosidases (analyzed in Ref. [10e]), are likely poor TS‡ mimics due to the significant energy barrier associated with interconversion to the $B_{2,5}$ conformation (a calculated FEL of IFG in solution shows $B_{2,5}$ to be approx-

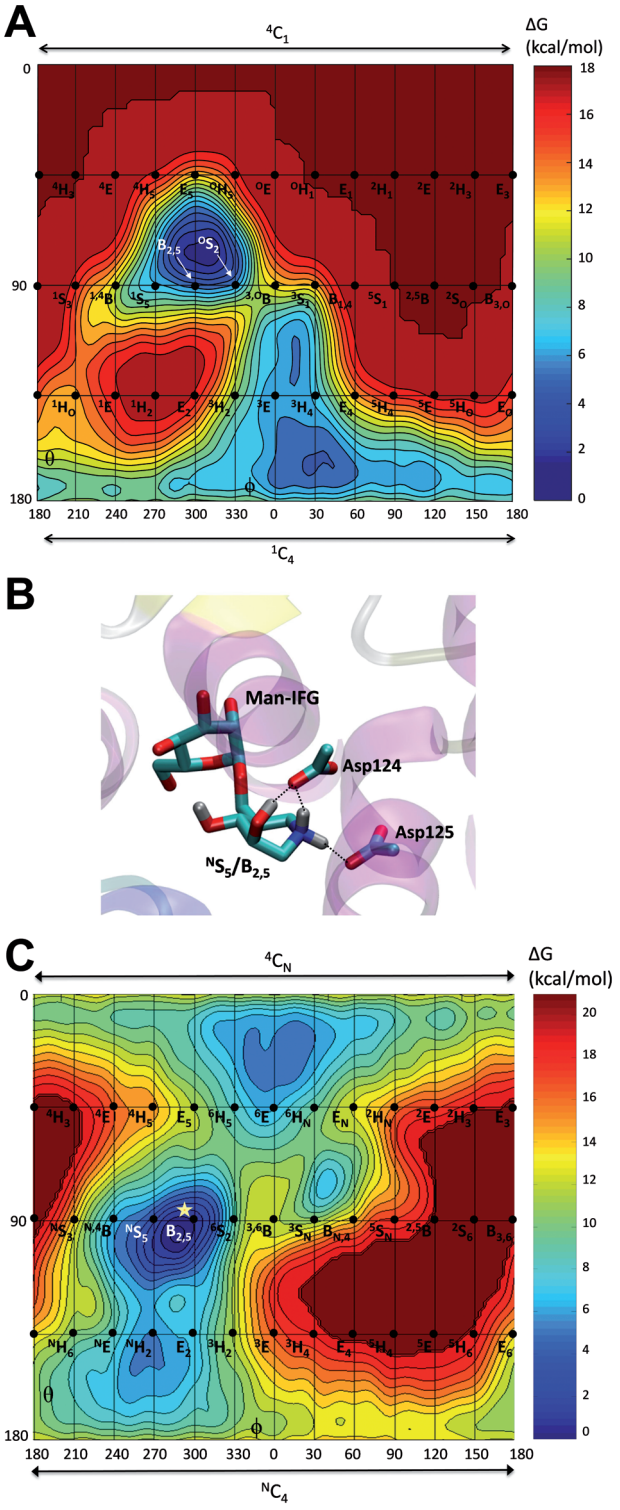

Figure 2. QM/MM metadynamics simulation of ligand binding to *Bc*GH76 α-1,6-mannanase. A) Conformational free-energy landscape (FEL) of the mannoside moiety at the −1 enzyme subsite within the α-1,6-mannopentaose complex. B) Complex with azasugar **3** with the lowest free energy. C) Conformational free-energy landscape (FEL) of the isofagomine moiety at the −1 enzyme subsite. FELs contoured at 1 kcal mol^{-1}. Star denotes the coordinates of the conformation from (B).

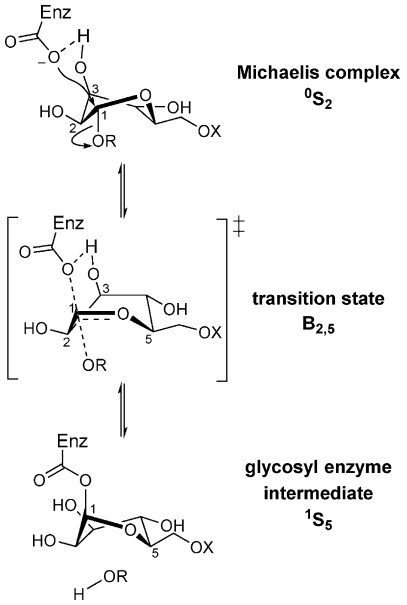

Figure 3. Proposed reaction coordinate for GH76 retaining α-mannanases via a $B_{2,5}$ $TS^{\ddagger}$. The deformed ground-state skew and transition-state boat conformations are stabilized through a direct interaction with the putative catalytic nucleophile (Asp124 for *Bc*GH76).

imately 8 kcal mol^{-1} higher in energy than $^4C_1$, with a barrier between the two of more than 10 kcal mol^{-1}).[10e] Exceptionally, a small number of IFG-type complexes with family GH6 cellulases[21] have been observed in $B_{2,5}$ conformations and this has been interpreted as evidence of a $B_{2,5}$ conformation for the $TS^{\ddagger}$ (for a detailed listing see SI), consistent with distortions observed in Michaelis complexes of the same family.[21] Rigorous analysis will be required to quantitatively assess the $TS^{\ddagger}$ mimicry of azasugar **3**; however, this work reveals that *Bc*GH76 is able to overcome the large intrinsic conformational bias of IFG, distorting the azasugar into a $B_{2,5}$ conformation and qualitatively recapitulating interactions and the conformation predicted for the $TS^{\ddagger}$. Fungal GH76 enzymes have been implicated in cross-linking of glycoproteins into the cell wall and GH76 genes *dcw1* and *dfg5* are involved in virulence within the pathogenic fungus *Candida albicans*,[2] suggesting that α-1,6-mannanase inhibitors may act as novel antifungal therapeutics. The present work reveals the first inhibitor for any GH76 enzyme, and key details of the conformational itinerary, catalytic residues, and unique interactions of the catalytic nucleophile with the 3-hydroxy group that may enable the development of antifungal $TS^{\ddagger}$-mimicking inhibitors.

Experimental Section

Crystals of *Bc*GH76 were grown as described in the Supporting Information (SI), with 3D structures determined using X-ray diffraction data collected at beamlines I04 and I04-1 of the Diamond Light Source (Didcot, UK). Further details regarding data processing, structure solution, and refinement are available from PDB headers and the SI. α-1,6-Mannanase activity was assessed using $pNPMan_2$ and α-1,6-M_3, as described in the SI. Thermodynamic studies of 1,6-ManIFG binding were determined at pH 7.0 and 25 °C using a MicroCal AutoiTC$_{200}$ calorimeter (Malvern Instruments). 1,6-ManIFG (450 μM) was titrated into the ITC cell containing 36 μM *Bc*GH76, and the K_d value calculated using the Origin 7 software package (MicroCal). QM/MM MD simulations were performed using a method that combines the Car-Parrinello MD, based on DFT, with force-field MD. The IFG moiety of the 1,6-ManIFG inhibitor and the α-mannoside at the −1 enzyme subsite were treated quantum-mechanically (QM region), whereas the rest of the substrate, the protein and the solvent (MM region) were treated with the AMBER force field. The PBE functional was used for the DFT calculations in view of its good performance on isolated sugars and carbohydrate-active enzymes. The metadynamics algorithm was used to explore the conformational free-energy landscapes of the IFG moiety of protonated **3** and the α-mannoside ring at the −1 enzyme subsite, taking as collective variables two of the puckering coordinates of Cremer and Pople (θ, ϕ) (see SI for further details and complete references).

Keywords: carbohydrates · computational chemistry · conformational analysis · enzymatic mechanisms · glycosidase inhibitors

How to cite: *Angew. Chem. Int. Ed.* **2015**, *54*, 5378–5382
Angew. Chem. **2015**, *127*, 5468–5472

[1] A. Helenius, M. Aebi, *Science* **2001**, *291*, 2364–2369.
[2] a) E. Spreghini, D. A. Davis, R. Subaran, M. Kim, A. P. Mitchell, *Eukaryotic Cell* **2003**, *2*, 746–755; b) H. Kitagaki, K. Ito, H. Shimoi, *Eukaryotic Cell* **2004**, *3*, 1297–1306.
[3] F. Cuskin, E. C. Lowe, M. J. Temple, Y. Zhu, E. A. Cameron, N. A. Pudlo, N. T. Porter, K. Urs, A. J. Thompson, A. Cartmell, A. Rogowski, B. S. Hamilton, R. Chen, T. J. Tolbert, K. Piens, D. Bracke, W. Vervecken, Z. Hakki, G. Speciale, J. L. Munoz-Munoz, A. Day, M. J. Pena, R. McLean, M. D. Suits, A. B. Boraston, T. Atherly, C. J. Ziemer, S. J. Williams, G. J. Davies, D. W. Abbott, E. C. Martens, H. J. Gilbert, *Nature* **2015**, *517*, 165–169.
[4] a) W. A. Lubas, R. G. Spiro, *J. Biol. Chem.* **1988**, *263*, 3990–3998; b) J. Roth, M. Ziak, C. Zuber, J. Roth, M. Ziak, C. Zuber, *Biochimie* **2003**, *85*, 287–294.
[5] V. Lombard, H. Golaconda Ramulu, E. Drula, P. M. Coutinho, B. Henrissat, *Nucleic Acids Res.* **2014**, *42*, D490–495.
[6] a) H. Kitagaki, H. Wu, H. Shimoi, K. Ito, *Mol. Microbiol.* **2002**, *46*, 1011–1022; b) A. Maddi, C. Fu, S. J. Free, *PLoS One* **2012**, *7*, e38872.
[7] C. Zuber, M. J. Spiro, B. Guhl, R. G. Spiro, J. Roth, *Mol. Biol. Cell* **2000**, *11*, 4227–4240.
[8] A. J. Thompson, R. J. Williams, Z. Hakki, D. S. Alonzi, T. Wennekes, T. M. Gloster, K. Songsrirote, J. E. Thomas-Oates, T. M. Wrodnigg, J. Spreitz, A. E. Stutz, T. D. Butters, S. J. Williams, G. J. Davies, *Proc. Natl. Acad. Sci. USA* **2012**, *109*, 781–786.
[9] S. Hiraizumi, U. Spohr, R. G. Spiro, *J. Biol. Chem.* **1993**, *268*, 9927–9935.
[10] a) L. E. Tailford, W. A. Offen, N. L. Smith, C. Dumon, C. Morland, J. Gratien, M. P. Heck, R. V. Stick, Y. Bleriot, A. Vasella, H. J. Gilbert, G. J. Davies, *Nat. Chem. Biol.* **2008**, *4*, 306–312; b) V. M. A. Ducros, D. L. Zechel, G. N. Murshudov, H. J. Gilbert, L. Szabó, D. Stoll, S. G. Withers, G. J. Davies, *Angew. Chem. Int. Ed.* **2002**, *41*, 2824–2827; *Angew. Chem.* **2002**, *114*, 2948–2951; c) S. Numao, D. A. Kuntz, S. G. Withers, D. R. Rose, *J. Biol. Chem.* **2003**, *278*, 48074–48083; d) Y. Zhu, M. D. Suits, A. J. Thompson, S. Chavan, Z. Dinev, C. Dumon, N. Smith, K. W. Moremen, Y. Xiang, A. Siriwardena, S. J. Williams, H. J. Gilbert, G. J. Davies, *Nat. Chem. Biol.* **2010**, *6*, 125–132; e) R. J. Williams, J. Iglesias-Fernandez, J. Stepper, A. Jackson, A. J.

Thompson, E. C. Lowe, J. M. White, H. J. Gilbert, C. Rovira, G. J. Davies, S. J. Williams, *Angew. Chem. Int. Ed.* **2014**, *53*, 1087 – 1091; *Angew. Chem.* **2014**, *126*, 1105 – 1109.
[11] a) K. Karaveg, A. Siriwardena, W. Tempel, Z. J. Liu, J. Glushka, B. C. Wang, K. W. Moremen, *J. Biol. Chem.* **2005**, *280*, 16197 – 16207; b) A. J. Thompson, J. Dabin, J. Iglesias-Fernandez, A. Ardevol, Z. Dinev, S. J. Williams, O. Bande, A. Siriwardena, C. Moreland, T. C. Hu, D. K. Smith, H. J. Gilbert, C. Rovira, G. J. Davies, *Angew. Chem. Int. Ed.* **2012**, *51*, 10997 – 11001; *Angew. Chem.* **2012**, *124*, 11159 – 11163.
[12] a) T. Nakajima, S. K. Maitra, C. E. Ballou, *J. Biol. Chem.* **1976**, *251*, 174 – 181; b) Y. Maruyama, T. Nakajima, *Biosci. Biotechnol. Biochem.* **2000**, *64*, 2018 – 2020.
[13] G. Speciale, A. J. Thompson, G. J. Davies, S. J. Williams, *Curr. Opin. Struct. Biol.* **2014**, *28*, 1 – 13.
[14] A. Striebeck, V. S. Borodkin, A. T. Ferenbach, D. M. F. Van Aalten, **2014**, unpublished PDB entry.
[15] G. J. Davies, K. S. Wilson, B. Henrissat, *Biochem. J.* **1997**, *321*, 557 – 559.
[16] G. J. Davies, A. Planas, C. Rovira, *Acc. Chem. Res.* **2012**, *45*, 308 – 316.
[17] S. McNicholas, E. Potterton, K. S. Wilson, M. E. Noble, *Acta Crystallogr. Sect. D* **2011**, *67*, 386 – 394.
[18] D. L. Zechel, S. G. Withers, *Acc. Chem. Res.* **1999**, *33*, 11 – 18.
[19] L. Petersen, A. Ardèvol, C. Rovira, P. J. Reilly, *J. Am. Chem. Soc.* **2010**, *132*, 8291 – 8300.
[20] M. Huang, G. E. Garrett, N. Birlirakis, L. Bohé, D. A. Pratt, D. Crich, *Nat. Chem.* **2012**, *4*, 663 – 667.
[21] a) A. Varrot, J. Macdonald, R. V. Stick, G. Pell, H. J. Gilbert, G. J. Davies, *Chem. Commun.* **2003**, 946 – 947; b) A. Varrot, S. Leydier, G. Pell, J. M. Macdonald, R. V. Stick, B. Henrissat, H. J. Gilbert, G. J. Davies, *J. Biol. Chem.* **2005**, *280*, 20181 – 20184.

Received: October 29, 2014
Revised: January 29, 2015
Published online: March 13, 2015

